Palacky University Olomouc

Faculty of Science

Department of Analytical Chemistry

Master´s thesis

Development of an analytical method for determination and identification of mescaline in plant and biological material

Lucie Skácelová

Supervisor: Assoc. Prof. RNDr. Vítězslav Maier, Ph.D.

Olomouc 2017

Univerzita Palackého v Olomouci

Přírodovědecká fakulta
Katedra analytické chemie

Diplomová práce

Vývoj analytické metody pro stanovení a identifikaci meskalinu v rostlinném a biologickém materiálu

Lucie Skácelová

Vedoucí práce: doc. RNDr. Vítězslav Maier, Ph.D.

Olomouc 2017

I hereby declare that this master´s thesis has been composed by myself autonomously under the supervision of Assoc. Prof. RNDr. Vítězslav Maier, Ph.D. All of the literary sources used in this work are listed in the references section.

In Olomouc ....

                                                               Lucie Skácelová

Bibliographic identification:

Author's first name and surname: Lucie Skácelová

Title: Development of an analytical method for determination and identification of mescaline in plant and biological material

Type of thesis: Master´s thesis

Department: Department of analytical chemistry

Supervision: Assoc. Prof . RNDr. Vítězslav Maier, Ph.D.

Year of presentation: 2017

Abstract: A new method for the identification and quantification of mescaline in plant and biological matrices, using capillary electrophoresis with mass spectrometry (CE-ESI-MS), was developed. For the plant samples, a simple extraction using ethanol, with basic pH adjusted by an addition of ammonium hydroxide (3%, *v/v*), was utilized. While no extraction was needed for the urine samples, it was necessary to dilute the samples ten times to minimize the influence of various salts and metabolites present within the matrix. The achieved limits of detection were 1.30 μg/l for the plant samples and 2.13 μg/l for the urine samples. This method is a fast, easy and effective alternative to the existing chromatographic methods.

Key words: mescaline, capillary electrophoresis, mass spectrometry, toxicological analysis

Number of pages: 49

Number of appendices: 0

Language: English

Bibliografická identifikace:

Jméno a příjmení autora: Lucie Skácelová

Název práce: Vývoj analytické metody pro stanovení a identifikaci meskalinu v rostlinném a biologickém materiálu

Typ práce: Magisterská práce

Pracoviště: Katedra analytické chemie

Vedoucí práce: doc. RNDr. Vítězslav Maier, Ph.D.

Rok obhajoby práce: 2017

Abstrakt: Byla vyvinuta nová metoda pro identifikaci a kvantifikaci meskalinu v rostlinných a biologických vzorcích, využívající kapilární elektroforézu s hmotnostní spektrometrií. Pro rostlinné vzorky byla použita jednoduchá extrakce etanolem o bazickém pH, které bylo upraveno přídavkem hydroxidu amonného (3%, *v/v*). U vzorků moči nebyla nutná extrakce, avšak bylo třeba vzorky desetkrát zředit, a to z důvodu potlačení vlivů solí a metabolitů přítomných v matrici. Získané limity detekce byly 1,30 µg/l pro rostlinné vzorky a 2,13 µg/l pro vzorky moči. Tato vyvinutá a optimalizovaná metoda je rychlou, jednoduchou a účinnou alternativou pro stávající chromatografické metody.

Klíčová slova: meskalin, kapilární elektroforéza, hmotnostní spektrometrie, toxikologická analýza

Počet stran: 49

Počet příloh: 0

Jazyk: Anglický

Table of contents

1. Introduction

Mescaline, a hallucinogenic alkaloid found in the majority of species of the *Lophophora* cactus, is classified as a controlled substance in both, the United States, where the cactus originates, and the Czech Republic. The use of this cactus, more precisely the mescaline within it, as a recreational drug has been reported to date back several thousand years. Its effects are comparable to those of other psychedelic drugs, namely LSD or psilocybin. Mescaline is a phenethylamine derivative and therefore it is structurally similar to a variety of drug classes, such as the nervous system stimulants (amphetamine).

Capillary electrophoresis (CE) is a rapidly developing analytical method that is becoming more popular due to its short analysis time and the low sample volumes required for the experiment. There are several sensitive detection techniques that make CE a good alternative to existing chromatographic methods. The electrospray ionization mass spectrometry (ESI-MS) detector offers low detection limits and fast response times, as well as valuable structural information about the analytes. However, the interface does have certain limitations, such as the need for volatile electrolytes or a sheath liquid to ensure optimal flow rates.

The aim of this thesis was to develop, optimize and validate a fast, easy and effective method for the determination of mescaline in plant and biological matrices, using capillary electrophoresis with mass spectrometry (CE-ESI-MS). The method was then utilized to measure the concentration levels of mescaline in over thirty plant samples.

The aims of this thesis were set as follows:

(i)   to develop and optimize a CE-ESI-MS method for the determination of mescaline – the optimization being carried out for both the CE and the MS parameters

(ii)   to validate the developed method using the following parameters: limit of detection, limit of quantification, linear dynamic range, correlation coefficient, accuracy (bias), intra-day and inter-day repeatability, recovery, matrix effect and process efficiency

(iii)   to prove the applicability of the developed method for the analysis of plant and biological samples

2. Theoretical part

2.1. Mescaline

2.1.1. Chemical and toxicological properties

Mescaline is a naturally occurring psychoactive hallucinogenic alkaloid primarily found in a genus of cacti by the name *Lophophora* J.M.Coult. There are several reported species of this plant, such as the *Lophophora alberto-vojtechii* J. Bohata*,* V. Myšák & J. Šnicer or the *Lophophora fricii* Haberm., however, the one with the highest amount of mescaline is the *Lophophora williamsii* (Lem. ex Salm-Dyck) J.M.Coult., also known as peyote.

Its systematic name, 3,4,5-trimethoxyphenylethylamine, suggests that mescaline is a phenethylamine derivative with the molecular formula $C_{11}H_{17}NO_3$ and the molecular weight of 211.258 g/mol, as is illustrated in Figure 1. It is soluble in benzene, chloroform and ethanol in addition to being moderately soluble in water. Since the melting point of mescaline is between 35 and 36 °C, it is generally synthesized in the form of a white crystalline powder, mescaline hydrochloride. [1–3].
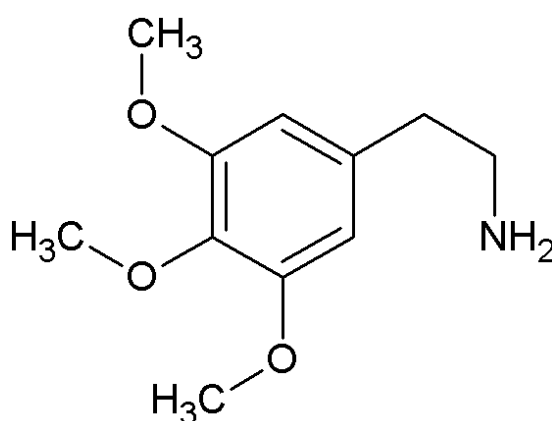
Figure 1: Structure of mescaline [4].

Mescaline is typically administered orally in the form of fresh or dried peyote buttons or a tea; however, it has a bitter, acrid taste which can induce nausea and vomiting if larger doses are ingested [5]. It acts as a partial agonist of the 5-HT$_{2a}$ receptors, which

play a role in neuropsychiatric disorders, such as schizophrenia, depression or panic disorder. It is used to treat infections, arthritis, asthma, influenza, intestinal disorders, diabetes, snake and scorpion bites, in addition to being reputed as an effective treatment of alcoholism [6–8]. Its mechanism of action is very similar to that of LSD and results in visual hallucinations, altered perception of self and reality, increased suggestibility and intensified emotions [1,6].

LSD is 4,000 times more potent than mescaline; however, the effects of mescaline are longer lasting. In humans the effects peak 2-4 hours after consumption and last for up to 12 hours, with 87% of the original dose being excreted in urine within 24 hours, either in an unchanged form or as the major metabolite 3,4,5- trimethoxyphenylacetic acid [2,9]. Depending on the dose, period of use and the sensitivity of the analytical method, mescaline can be found in urine for 1-4 days after ingestion, while past exposure can be determined using hair samples. The hallucinogenic doses typically range from 200 to 500 mg of mescaline, which is equivalent to about 5 g of dried peyote [10].

2.1.2. Peyote

While there are many mescaline-containing cacti, such as the San Pedro (*Trichocereus pachanoi* Britton & Rose) or the Peruvian torch (*Trichocereus peruvianus* Britton & Rose), the one most commonly associated with mescaline is peyote (*Lophophora williamsii*). *Lophophora williamsii* is classified as a Schedule I illicit substance and is considered illegal in the United States, except for the 300,000 members of the Native American Church (NAC), who are permitted the "sacramental use" of peyote for religious practices [5,8]. There is evidence of ceremonial use of peyote dating back to 5,700 years ago [11,12].

Peyote, also known as "devil´s root", "dumpling cactus", "mescal button" and "sacred mushroom", can be mainly found on limestone hills and in other calcareous soils in the desert area of Mexico and in smaller quantities on the US side of the Texas-Mexico border, as is shown in Figure 2. It is an extremely slow growing, small (4-12 centimetres in diameter), spineless, blue-green, button-like cactus composed of three identifiable parts shown in Figure 3 – the crown, the non-chlorophyllous stem and the root [5,8,13].
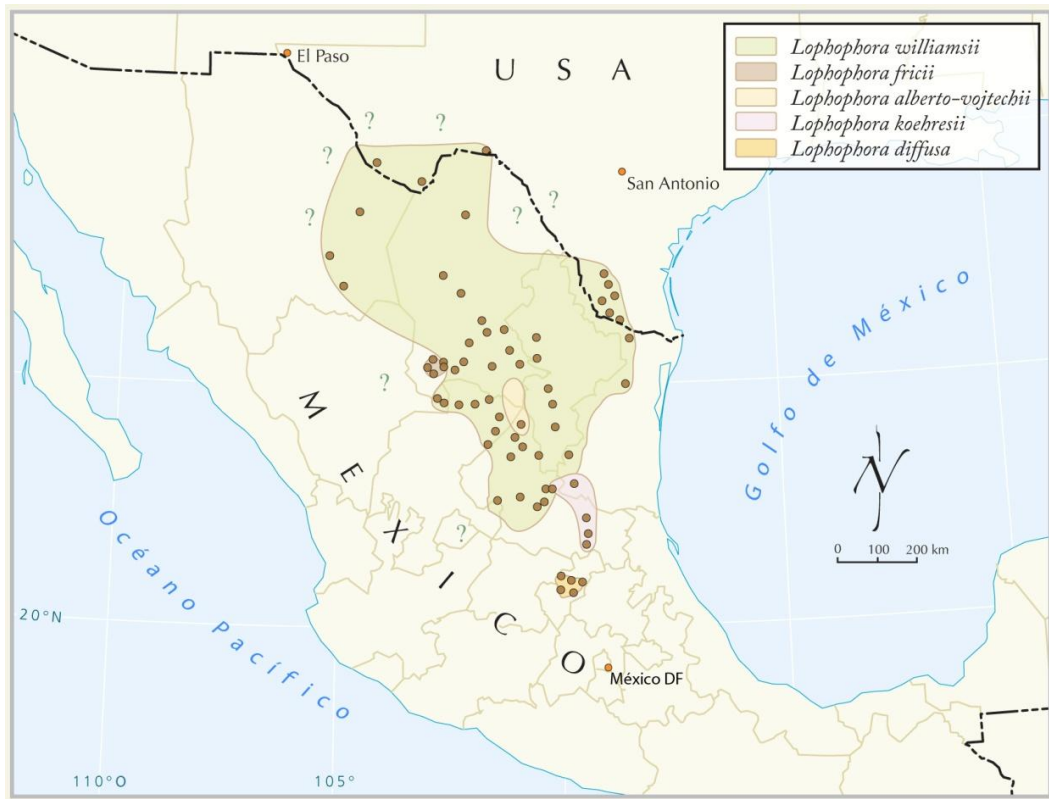
Figure 2: A map of the approximate location range of the *Lophophora* plant (2008), color coded for the different species with the exact locations shown by dots [14].
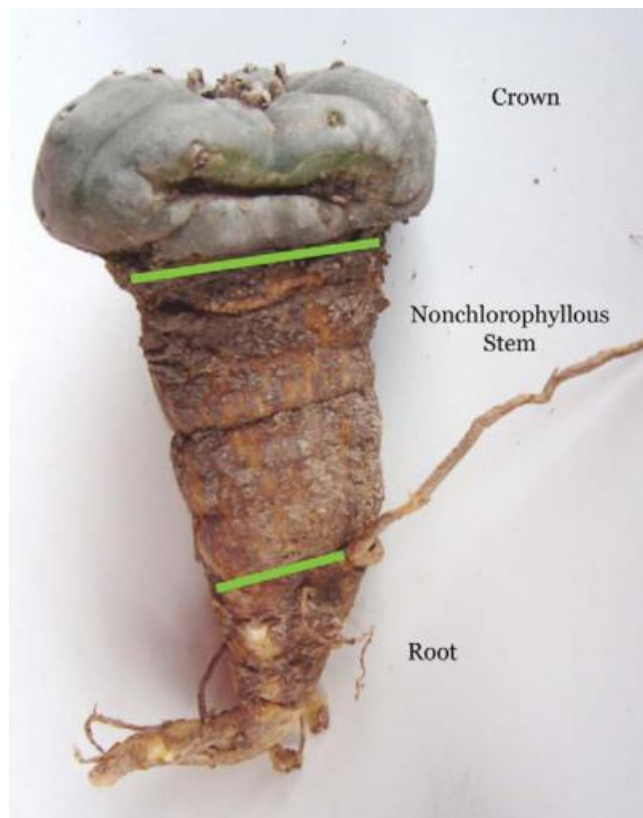
Figure 3: *Lophophora williamsii* mature adult [13].

A study regarding the varying concentrations of mescaline in the three principal tissues of the peyote cactus showed that the mescaline concentration in the crown of the plant ranged from 2 to 4% of the dry weight of the crown. As expected, the non-chlorophyllous stem contained concentrations an order of magnitude lower while the root contained the lowest concentrations – two orders of magnitude lower than in the crown tissue [13].

2.1.3. Biosynthesis of mescaline

Mescaline is structurally related to the methylated derivatives of the catecholamine neurotransmitters, dopamine and norepinephrine. As seen in Figure 4, the metabolic precursors of the synthesis are hydroxylated phenylalanine or tyrosine. The key step is the correct methylation of the hydroxyl groups, otherwise the biosynthesis may lead to the formation of the isoquinoline alkaloids anhalonidine and anhalonine [15,16].
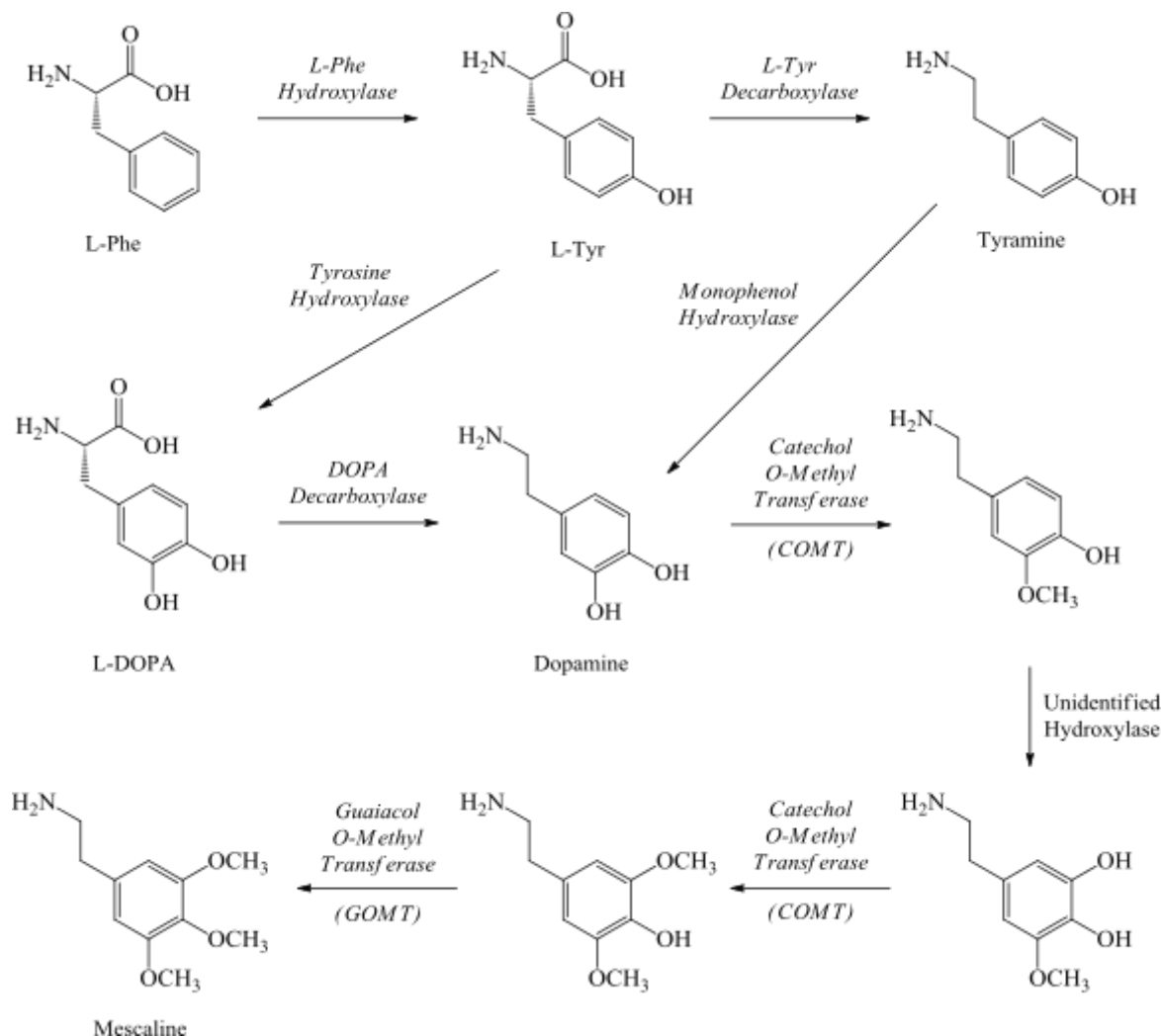
Figure 4: Pathways in the in-vitro formation of mescaline [15].

2.1.4. Analytical methods for mescaline assay

While mescaline is the principal constituent in the peyote cactus, there are over 60 additional alkaloids, such as lophophorine, anhalonine, pellotine or anhalonidine, which can be found in the plant. Since the typical usage of peyote is in the form of the dried tops of the plant, so called "peyote buttons", a whole range of alkaloids can be found in the plant and biological samples [5,12]. Therefore a wide selection of separation methods has been developed for the analysis of mescaline, as shown in Table 1.

In addition, the information contained within Table 1 comparatively shows the wide range of analytical methods, including sample preparation and detection, used for the determination of mescaline in varying matrices. To each method there are certain advantages and disadvantages; for example, an important step in the sample preparation for the gas chromatography (GC) analysis is derivatization, which is not needed when the liquid chromatography (LC) methods are applied. On the other hand the primary amine group of mescaline readily adsorbs onto various types of LC stationary phases, such as the silica gel or other stationary phases with free silanol groups. Alternatively, there are differences between the used methods of detection. The two most commonly utilised detection methods are the non-destructive UV detection (PDA/DAD) and the destructive mass spectrometry (MS); however, MS detection severely overshadows UV detection in terms of the frequency of use. Whilst both have certain advantages, MS detection allows for additional positive identification of the separated substances.

Table 1: A summary of methods used for the analysis of mescaline.

Method	Material	Sample Preparation	Conditions	LOD/LOQ	Injection volume	References
GC-MS	Plasma	SPE, derivatization with HFBA, internal STD[1]	HP-5 MS capillary, T gradient, splitless, He carrier gas, EI	LOQ 5 μg/l	1 μl	[17]
HPLC-DAD	Plant	lyophilisation, pulverization, defattening, extraction: methanol-ammonia, internal STD	T = 25°C, acetonitrile-water	LOD 0.04 μg/mg	5 μl	[18]
GC-MS	Urine	internal STD, defattening, drying, derivatization HFBA	capillary column, T gradient, HP1, He carrier gas, SIM	LOD 100 ng/ml if 1ml of specimen analyzed	1 μl	[19]
HPLC-MS-MS	Oral Fluid	μ-SPE (OMIX C18 tips), internal STD	RP C18, acetonitrile-water	LOD 0.07 ng/ml, LOQ 0.2 ng/ml	Not mentioned	[20]
LC-MS-MS	Urine	SPE (C18), internal STD, drying	RP C18, methanol gradient in ammonium acetate buffer	LOD 3-5 μg/l	10 μl	[2]
GC- MS	Blood	internal STD, pH adjustment, LLE, drying	HP-1 column, T gradient	Not mentioned	2 μl	[9]
LC-PAD	Plant	drying, pulverization, defattening, extraction: methanol-concentrated ammonia	C18, T = 25°C, water-acetonitrile, λ = 268 nm	LOD 0.28 μg, LOQ 1.40 μg of mescaline	20 μl	[4]

---

[1] Mescaline-d_9 – deuterated internal standard [2].

Method	Material	Sample Preparation	Conditions	LOD/LOQ	Injection volume	References
NACE - EC (UV)	Standard	Not mentioned	acetonitrile buffer solution (sodium acetate + acetic acid), detection: Pt microdisk electrode (+1.8V); UV λ = 210 nm	LOD 3.9 μg/ml (UV detection LOD 2.2 μg/ml)	Not mentioned	[21]
Ion-interaction HPLC	Plant	grinding, extraction: methanol-ammonium solution or phosphate buffer	RP C18, octylamine o-phosphate, λ = 230 nm	LOD 35 μg/ml	Not mentioned	[22]
GC-MS	Plant* (archaeological sample)	pulverization, extraction: ethanol, filtration, oily residues dissolved in water, pH adjustment, extraction: chloroform then chloroform : ethanol (3:1), drying, filtration, evaporation	HP-5 MS capillary, EI, injector T = 200°C, column T = 100°C for 1 min then increased to 250°C (30°C/min) *TLC: silica gel, chloroform m: butanol: concentrated ammonia (50:50:2,5); ninhydrin → purple; iodoplatinate - Dragendorff's reagent → brownish-purple*	Not mentioned	2 μl	[12]
		HCl addition, boiling water bath (15 min), filtration, extraction: diethylether, centrifugation, drying, filtration, evaporation				

Method	Material	Sample Preparation	Conditions	LOD/LOQ	Injection volume	References
GC-MS	Liquid sample, Urine	internal standard, pH adjustment, extraction: dichloromethane : isopropanol (9:1), centrifugation, organic phase evaporated under nitrogen stream, derivatization (PFPA/PFPOH), evaporation, reconstitution with ethyl acetate	EI, ion trap, SPB-35 capillary, injector T = 250°C, T gradient, splitless, He carrier gas	Not mentioned	1 μl	[10]
GC-MS-MS	Hair	decontamination (dichloromethane), drying, cutting into small segments, internal standard, hydrolysis (HCl), cooling, pH adjustment, extraction: dichloromethane : isopropanol (9:1), derivatization (PFPA/PFPOH), evaporation, reconstitution with ethyl acetate		LOD 50 pg/mg	1 μl	
ELISA	Hair	decontamination (methanol), incubation, decantation, extraction (methanol), heating, cooling, evaporation, reconstitution with phosphate buffer	Single step ELISA kit for amphetamines, microwells coated with a high affinity capture antibody to the desired drug, λ = 450 nm	LOD 60 pg/mg	20 μl	[23]

2.2. Capillary electrophoresis

2.2.1. Method principle

Capillary electrophoresis (CE) is an analytical separation method, based on the different electrophoretic mobility of charged particles in an electric field. It can be used for the separation of various types of analytes, such as amino acids, chiral drugs, vitamins, pesticides, inorganic ions, organic acids, dyes, surfactants, carbohydrates or peptides and proteins. Hydrophobic or neutral analytes can be measured using micellar electrokinetic chromatography [24].

The main advantages of CE lay in its diverse application range, minimal sample volume requirements, the lack of organic waste, as well as oftentimes simpler method development in comparison to chromatographic methods. In addition, the surface-to-volume ratio of the capillary allows for the dissipation of the Joule heat generated from the applied electric field. The high electrical resistance of the capillary permits the use of very high potentials (up to 30 kV), resulting in short analysis times and high efficiency and resolution [24,25].

The term electrophoretic mobility μ_{ep} is used to describe the movement of a charged particle in an electric field. Together with the electric field strength E, it determines the electrophoretic velocity v_{ep} of the charged particle (1) [24].

$$v_{ep} = \mu_{ep}E \qquad (1)$$

The electric field strength is then defined as the applied voltage U divided by the length of the entire capillary L (2) [26].

$$E = \frac{U}{L} \qquad (2)$$

With the application of the electric field, the particles start to move to the electrodes with an opposite polarity, while under the influence of the electric force F_e. The electric force F_e is directly proportional to the ion charge q and the electric field strength E (3). The movement of the particles is slowed down by the frictional force F_f, which is described by Stoke´s law (for a spherical ion) as directly proportional to the ion charge q, solution

viscosity η, ion radius r and ion velocity v_{ep} (4) [24].

$$F_e = qE \qquad (3)$$
$$F_f = 6\pi\eta r v_{ep} \qquad (4)$$

Since the opposite forces have an equal value when in a steady state (5), the electrophoretic mobility can also be expressed as being directly proportional to the ion charge q, while being indirectly proportional to the solution viscosity η and ion radius r (6). It can therefore be said, that small particles with a large ion charge will move faster than large particles with small ion charge. Since viscosity is highly temperature dependent (viscosity decreases with increasing temperature), the electrophoretic mobility is also influenced as it will increase with increasing temperature [24,26].

$$F_e = -F_f \qquad (5)$$
$$\mu_{ep} = \frac{q}{6\pi\eta r} \qquad (6)$$

2.2.2. Electroosmotic flow (EOF)

Another phenomenon adding to the movement of particles in electrophoresis is the electroosmotic flow (EOF), a direct consequence of the surface charge on the wall of the uncoated fused-silica capillary. The silanol (Si-OH) groups (pK_a 3-5) present on the capillary inner surface can lead to the formation of silanate ions (SiO-), depending on the buffer pH. These negatively charged ions then allow for the adsorption of ions with an opposing charge (cations), leading to the formation of a fixed (Stern) layer, while some ions can be more loosely bound and form an outer mobile layer, as is shown in Figure 5. The fixed and the mobile layers are together called the double layer, and are responsible for the formation of a potential difference called the *zeta* potential ζ. When voltage is applied, the solvated cations in the outer layer migrate toward the cathode pulling along the solution and therefore forming the electroosmotic flow [24,27,28].
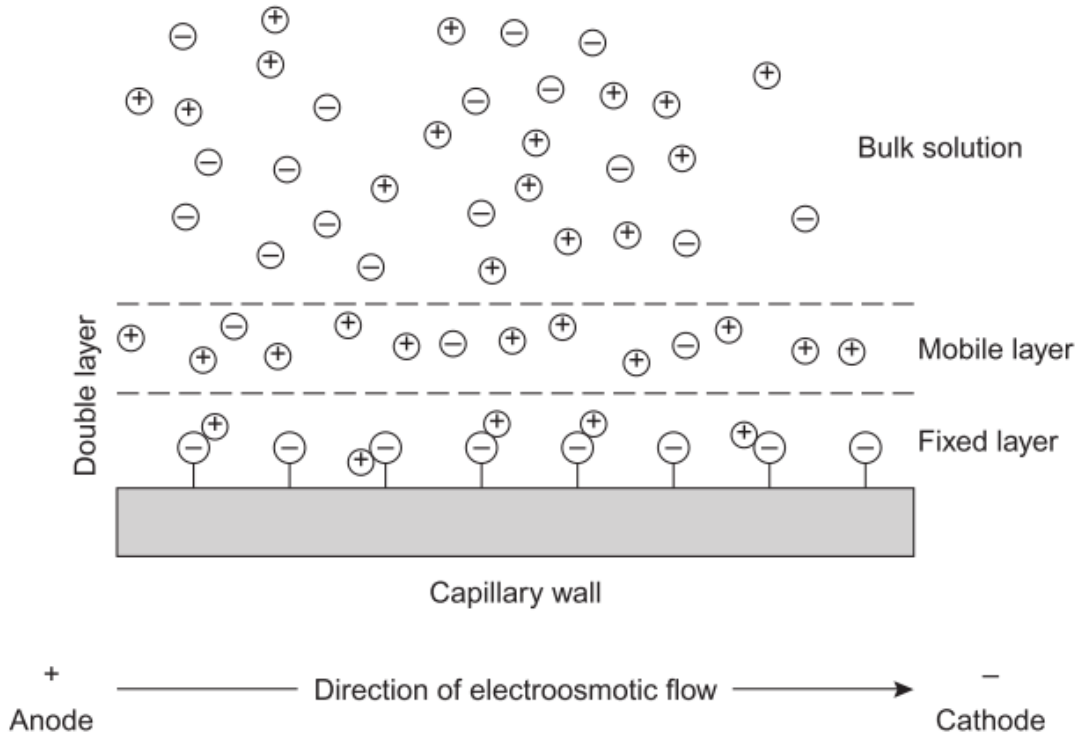
Figure 5: Schematic diagram showing the origin of electroosmotic flow [27].

Electroosmotic flow velocity v_{eof} is defined as the velocity with which the solute moves through the capillary due to the electroosmotic flow, and can be expressed as the function of the electric field strength E and the electroosmotic mobility μ_{eof} of solution (7). The electroosmotic mobility is then directly proportional to the dielectric constant of the solution ε and the *zeta* potential ζ, and indirectly proportional to the solution viscosity η (8) [27].

$$v_{eof} = \mu_{eof}E \qquad (7)$$

$$\mu_{eof} = \frac{\varepsilon\xi}{4\pi\eta} \qquad (8)$$

As previously mentioned, the *zeta* potential is determined by the surface charge on the capillary wall, which is largely pH dependent, therefore, the value of the electroosmotic mobility varies with changing pH. The *zeta* potential is also influenced by the buffer ionic strength, as an increase in ionic strength causes a decrease in zeta potential and therefore the electroosmotic mobility [29].

While the presence of EOF is in most cases beneficial, it generally needs to be controlled. For example, rapid EOF, a result of high pH, might cause an elution of analytes

before separation even had the chance to occur. The parameters that can be used to control EOF are summarised in Table 2 [29].

Table 2: Parameters controlling EOF [24].

Variable	Result	Comment
Electric field	EOF changes proportionally with electrical field	Generates Joule heat
Buffer pH	EOF decreases with lower pH and vice versa	May change solute charge
Ionic strength or buffer concentration	EOF increases at low ionic strength	High ionic strength generates high current (Joule heat)
Temperature	EOF changes due to viscosity change (2-3%/°C)	Thermostated capillary
Neutral hydrophilic polymer	Decreases and controls EOF, shields surface charge, increases viscosity	Adsorbs to capillary wall (hydrophilic interactions)
Organic modifiers	Changes zeta potential and electrolyte viscosity	Complex changes of EOF
Additives (surfactants)	Change magnitude and direction of EOF	Dynamic adsorption to capillary wall (hydrophobic/ionic)
Covalent bonded surface coating	EOF changes depending on the charge and polarity of the coating	Many possible modifications

Thanks to the small dimensions of the capillary, the velocity of a liquid is nearly uniform across the capillary inner diameter, resulting in a flat flow velocity profile called the "plug flow", as is shown in Figure 6b. In comparison, in the systems where the flow is caused by a pressure differential, the flow velocity profile presents as laminar, as seen in Figure 6a, oftentimes causing undesired band broadening [24,30].
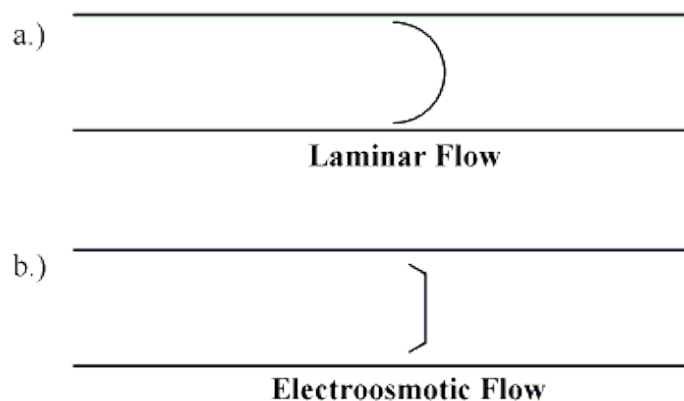
Figure 6: The comparison of the a) laminar (HPLC) and b) electroosmotic (CE) flow velocity profiles [24].

2.2.3. Instrumentation

Another advantage of CE is its simplistic instrumentation. The main components, as seen in Figure 7, are the fused silica capillary, placed between the outlet and inlet buffer reservoirs, electrodes connected to a high voltage power supply, controlled by the computer software, and the detector. Sample injection is carried out by replacing one of the buffer reservoirs with a sample reservoir and applying either an electric field (electrokinetic injection) or external pressure (hydrodynamic injection) [24].

Additionally, the capillary is thermostated to ensure measurement repeatability as well as suitable efficiency [31].
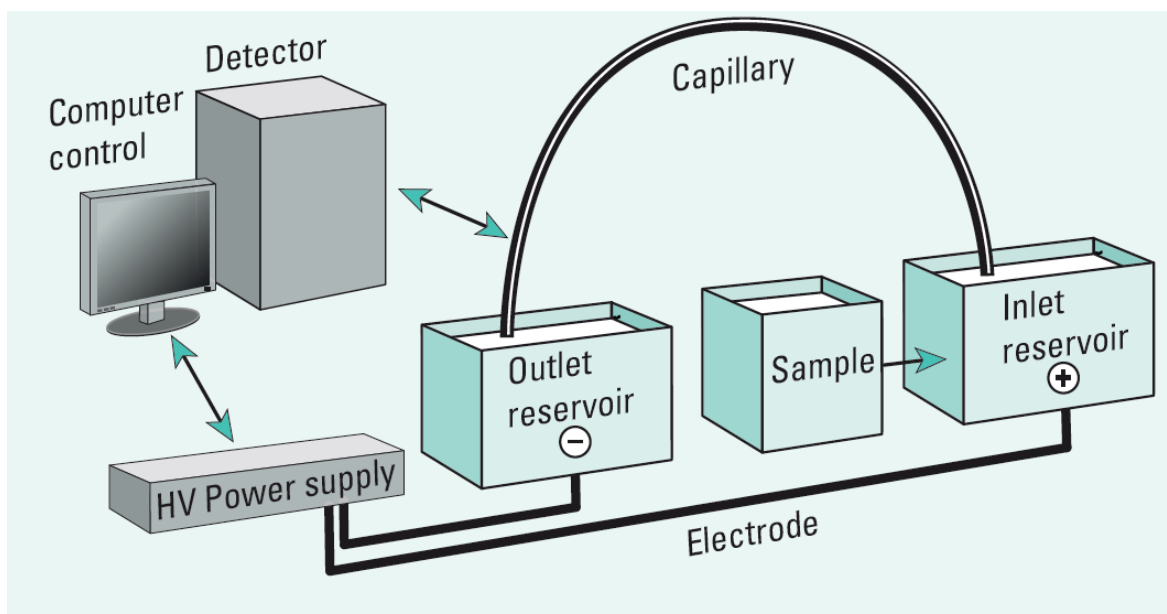
Figure 7: Basic components of CE instrumentation [24].

2.2.5. Detectors

The method of detection is generally selected in accordance with the type of analyte. While the UV/Vis detection is quite possibly the most common, the required presence of a chromophore severely limits its range of application. Moreover, when compared to other methods, its sensitivity is among the lowest. The most frequently utilized detection methods are summarized in Table 3.

Table 3: The characteristics of selected detection methods for CE [24,27].

Detector	Selectivity	LOD (mol/l)
UV/Vis absorbance	Analytes with chromophore	10^{-5}-10^{-7}
Indirect absorbance	Universal	10^{-4}-10^{-6}
Fluorescence	Sensitive (derivatization)	10^{-7}-10^{-9}
Laser fluorescence (LIF)	Extremely sensitive (derivatization)	10^{-13}-10^{-16}
Amperometry	Selective for electroactive analytes	10^{-7}-10^{-10}
Conductivity	Universal	10^{-7}-10^{-9}
Radiometric	Radioactive analytes	10^{-10}-10^{-12}
Mass spectrometry	Universal	10^{-8}-10^{-10}

2.2.6. Capillary electrophoresis with mass spectrometry

Capillary electrophoresis with mass spectrometry detection (CE-MS) allows for the separation and detection of compounds at low LODs in addition to offering the possibility of analyte identification. The CE-MS system combines the advantages of the capillary electrophoresis, especially its separation effectiveness, with a selective and sensitive detection. As for example, analytes with the same molecular weight cannot be distinguished by MS, however, they are easily separated by CE. Vice versa, analytes coeluting in CE can be distinguished in MS, due to their varying molecular weight and dissimilar fragmentation [24,32].

Electrospray ionization

The CE-MS system requires for the molecules of the analyte to be transferred from the separation capillary to the mass spectrometer via an interface. Out of the wide range of ionization techniques, the only ones suitable for the CE-MS system, are the atmospheric pressure ionization techniques, such as the electrospray ionization (ESI), the atmospheric pressure chemical ionization (APCI), the atmospheric pressure photoionization (APPI) and the matrix-assisted laser desorption ionization (MALDI). Electrospray ionization is the method of choice for the transfer of ionic molecules from the liquid into the gas phase, due to its versatility, ease of use and effectiveness for charging large biomolecules. Figure 8 shows a diagram of electrospray ionization [33–35].

Figure 8: A diagram describing the electrospray ionization process [24].

Due to the CE flow rates (nl/min) being insufficient for maintaining a stable electrospray, the CE-ESI-MS requires the presence of a flowing sheath liquid – typically an aqueous mix of volatile organic solvents such as methanol or acetonitrile with acidic or basic additives (depending on the character of the analyte) [24,35]. The sheath flow sprayer instrumentation can be seen in Figure 9.

Figure 9: A schematic of a CE-MS sheath flow sprayer [24].

The electrospray ionization principle is as follows: the eluate leaving the end of the capillary undergoes nebulisation and forms very small electrically charged droplets, which then decrease in size due to solvent evaporation until they reach a point where the electrostatic repulsion overcomes cohesion and the droplets explode (coulombic fission) into a number of smaller stable droplets. The process is repeated until only gaseous ionic molecules remain [24,34].

The quadrupole analyzer

The quadrupole analyzer consists of four cylindrical metal rods, set parallel to each other, to which direct current and RF voltages are applied. The analyte ions are directed down the centre of the rods, where they start to oscillate. Only analytes with a specific *m/z* value can pass through the analyzer onto the detector. The other ions remain undetected as they lose their charge through a collision with one of the rods. A schematic representation of the quadrupole analyzer can be seen in Figure 10 [36].
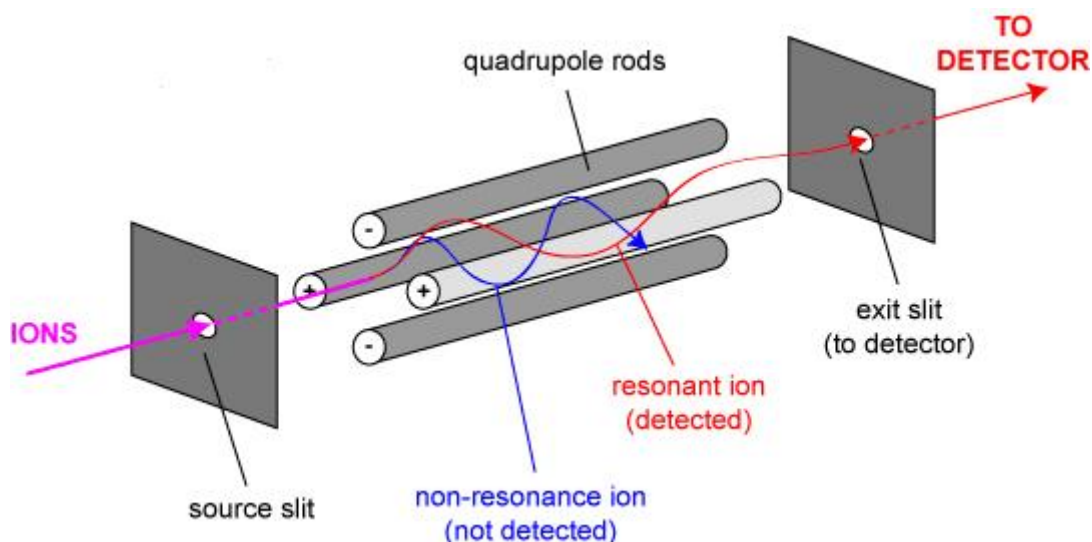
Figure 10: Quadrupole analyzer [37].

The triple quadrupole (QqQ) consists of a linear series of three quadrupoles and is typically utilized for a quantitative analysis. The middle quadrupole (q_2), filled with collision gas, performs the function of a collision cell as it causes collision induced dissociation of ions chosen by the first quadrupole (Q_1), which is a mass filter. The formed fragments are then analyzed by the third quadrupole (Q_3), also a mass filter.

The triple quadrupole can operate in scan mode, analyzing a selected range of *m/z* values and providing a complete picture of all the ionized compounds present (above LOD). As such, the full scan analysis is used for sample characterization and is a starting point for further method development. To increase method sensitivity, the quadrupole can operate in a selected ion monitoring mode (SIM), which narrows down the analysis to only a few specific *m/z* values. The method sensitivity is significantly improved as the quadrupole spends more time sampling each of these chosen *m/z* values. The quadrupole analyzer can also be used for the detection of fragmentation products through the selected reaction monitoring (SRM) method. Alternatively, the multiple reaction monitoring (MRM) method is used for the simultaneous detection of several fragmentation products from one or more precursor ions [36,38].

3. Experimental part

3.1. Materials and methods

3.1.1. Chemicals

Sample solutions of mescaline were prepared from stock solutions of mescaline standard (1 mg/ml) and deuterated mescaline-d_9 standard (0.1 mg/ml). The following chemicals were used for the preparation of the sheath liquid, the running buffer and the extraction mixture: methanol, ethanol (of LC-MS grade), formic acid ($\geq$95%, *w/v*), acetic acid ($\geq$96%, *w/v*), ammonium hydroxide (25%, *w/v*) and deionised water. The deionised water was prepared using a water purification system (18 MΩ, Millipore, Mohlsheim, France). Sodium hydroxide solution (0.1 M) was used for capillary conditioning. All chemicals were purchased from Sigma-Aldrich (St. Louis, MO, USA).

Unless stated otherwise, all of the aforementioned materials were of analytical grade.

3.1.1. Apparatus

All experiments were performed utilizing capillary electrophoresis system Agilent 7100 (Agilent Technologies, Waldbronn, Germany) coupled with tandem mass spectrometry Agilent 6460 with electrospray ionization and triple quadrupole analyser. An Agilent G1310 LC isocratic pump supplied the sheath liquid needed for electrospray ionization through a 1:100 flow splitter.

The analyses were carried out using an uncoated fused silica capillary (70 cm x 50 μm I.D.), which was conditioned with 0.1 M sodium hydroxide for 10 minutes, followed by deionised water for 10 minutes and finally the running buffer for 10 minutes. The capillary was flushed with the running buffer for 2 minutes before each analysis. Further experimental conditions are summarized in Table 4.

Table 4: Summary of optimal experimental conditions.

Optimal experimental conditions	
Buffer	25mM ammonium acetate, pH 3.5
Sample injection	100 mbar/5 s
Separation voltage	+ 25 kV
MRM	Mescaline-d$_9$ 221.3 → 204.3 (qualifier 204.3) Mescaline 212.3 → 195.3 (qualifier 181.1)
Collision energy	4 eV
Fragmentor voltage	100 V
Gas temperature	350 °C
Gas flow	10 l/min
Sheath liquid flow	4 μl/min
Sheath liquid composition	MeOH : W : FA (50:49.5:0.5% *v/v/v*)
Nebulizer	10.0 psi
Spraying voltage	+ 3.5 kV

3.2. Sample preparation

3.2.1. Plant samples

For the purpose of determination of mescaline in plant material, more than thirty different cacti samples, grown in the Czech Republic, were donated by the Palacky University Department of Botany. The samples ranged from 4 to 6 cm in size and were kept frozen prior to analysis. The plants were dried to constant weight at 105 °C and thoroughly crushed in a mortar. An exact amount (100.00 mg) of the desiccated plant matter was transferred into a flask and extracted in a sonic bath, thermostated at 25 °C, for 10 minutes using 5 ml of ethanol, with a basic pH adjusted by an addition of ammonium hydroxide (3%, *v/v*). Following the filtration of the extracts through a 45 μm disc syringe filter, aliquots of 0.1 ml were dried under a stream of nitrogen and reconstituted using 1 ml of deionised water. The quantification of mescaline in the plant samples was ensured, by an addition of the mescaline-d$_9$ standard.

3.2.2. Urine samples

Due to the lack of a genuine clinical sample, the analysis was performed on urine not containing mescaline. The urine was diluted ten times with water and was spiked with calculated amounts of the mescaline and mescaline-d$_9$ standards. The samples have

undergone no further alterations before injection. A sample of the diluted urine was analysed independently to ascertain the presence of metabolic interferences, of which none have been found.

3.3. Experimental conditions optimization

Buffer concentration and buffer pH optimization

The utilization of MS as a detector makes the usage of volatile buffers a necessity. The properties of the buffer, such as pH and ionic strength, majorly impact the protonization of the analyte and the rate of adsorption of the protonized analyte onto the silica capillary inner wall. Considering mescaline migrates as a cation (pK_a 9.5 [39]), acidic running buffers are the most suitable choice for the analysis.

The running buffer was prepared by diluting an appropriate amount of acetic acid with deionised water, followed by an ammonium hydroxide titration to reach a desired pH value. The ammonium acetate was chosen for the separation, as the other available option - ammonium formiate, produced lower peak area and migration time repeatability. The experiment was carried out using three different buffer concentrations, 10 mM, 25mM and 50 mM ammonium acetate (Figure 11) and six different pH values, 3.5, 4.0, 4.5, 5.0, 5.5 and 6.0 (Figure 12). The aim was to find a compromise between the largest intensity and the shortest migration time. Taking into account the standard deviations of the measurements, the optimal running buffer parameters were chosen to be the 25 mM ammonium acetate concentration and the pH 3.5.
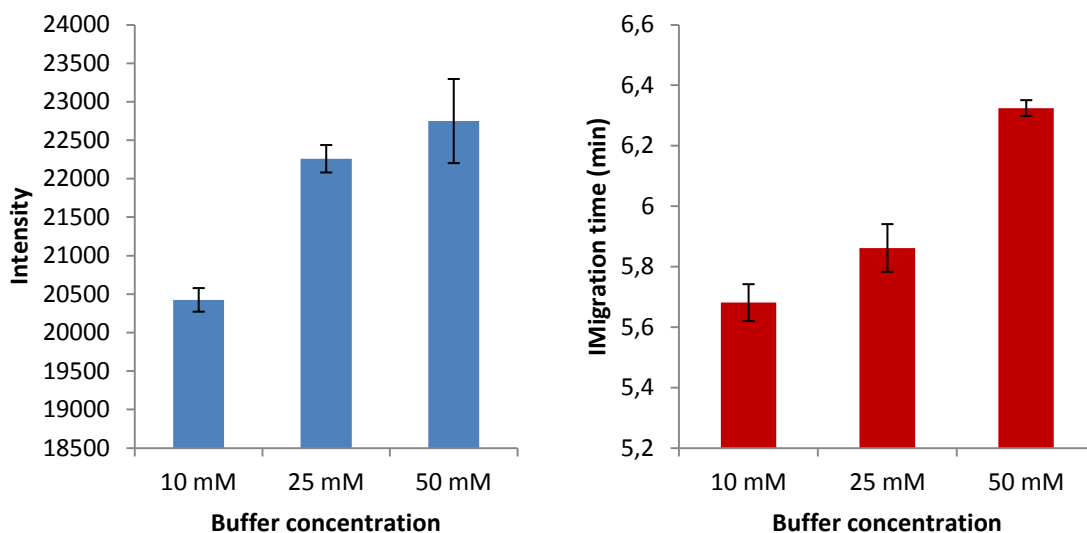
Figure 11: The dependence of intensity (blue) and migration time (red) on buffer (ammonium acetate) concentration, measured for a sample of 5 mg/l mescaline in water.
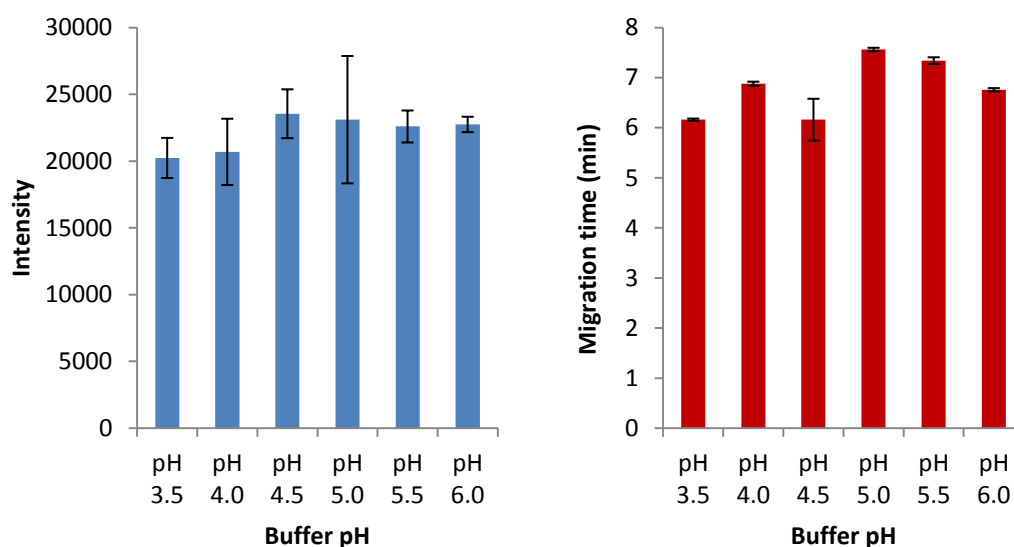
Figure 12: The dependence of intensity (blue) and migration time (red) on buffer (ammonium acetate) pH, measured for a sample of 5 mg/l mescaline in water.

Collision energy optimization

In order to ascertain the optimal conditions for the analysis, several different MS parameters were investigated, starting with collision energy. The aim was to find such collision energy value that would result in a sufficient fragmentation of the precursor ion [Mescaline+H]$^+$ whilst ensuring the highest abundance of the product ions. The presence of the precursor ion is required for irrefutable positive identification of the analyte. To

further confirm the outcome, a qualifier ion, a product ion with the second highest abundance (if present), was chosen for both the mescaline and the mescaline-d$_9$ standard. The experiment was carried out with the collision energy value set at 2, 3, 4, 5, 6 and 10 eV. Figure 13 illustrates the complete fragmentation of the precursor ion at 10 eV, while Figures 14 and 15 show the product spectra for the chosen optimal collision energy value of 4 eV for mescaline and mescaline-d$_9$ respectively. The neutral loss of ammonia (Δ *m/z* = 17) can be seen in both Figure 14 and Figure 15.

This experiment was performed for both the mescaline and mescaline-d$_9$ standards. The product ions with the highest abundance were subsequently chosen for the multiple reaction monitoring (MRM) acquisition method.
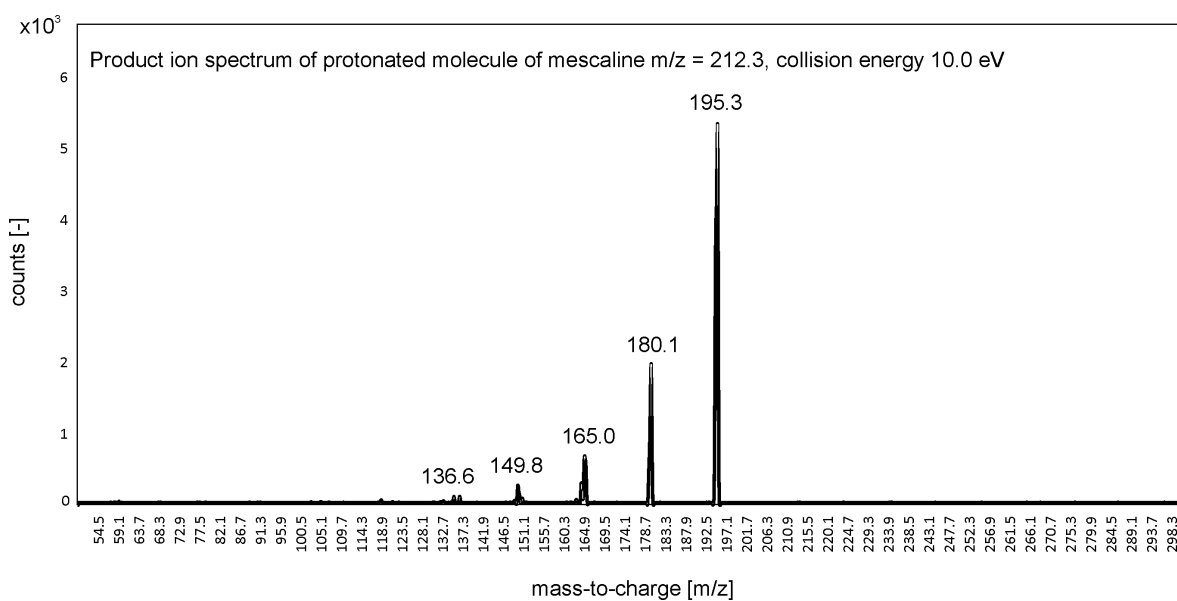
Figure 13: Product ion spectrum measured for a sample of 5 mg/l mescaline in water, collision energy at 10 eV.
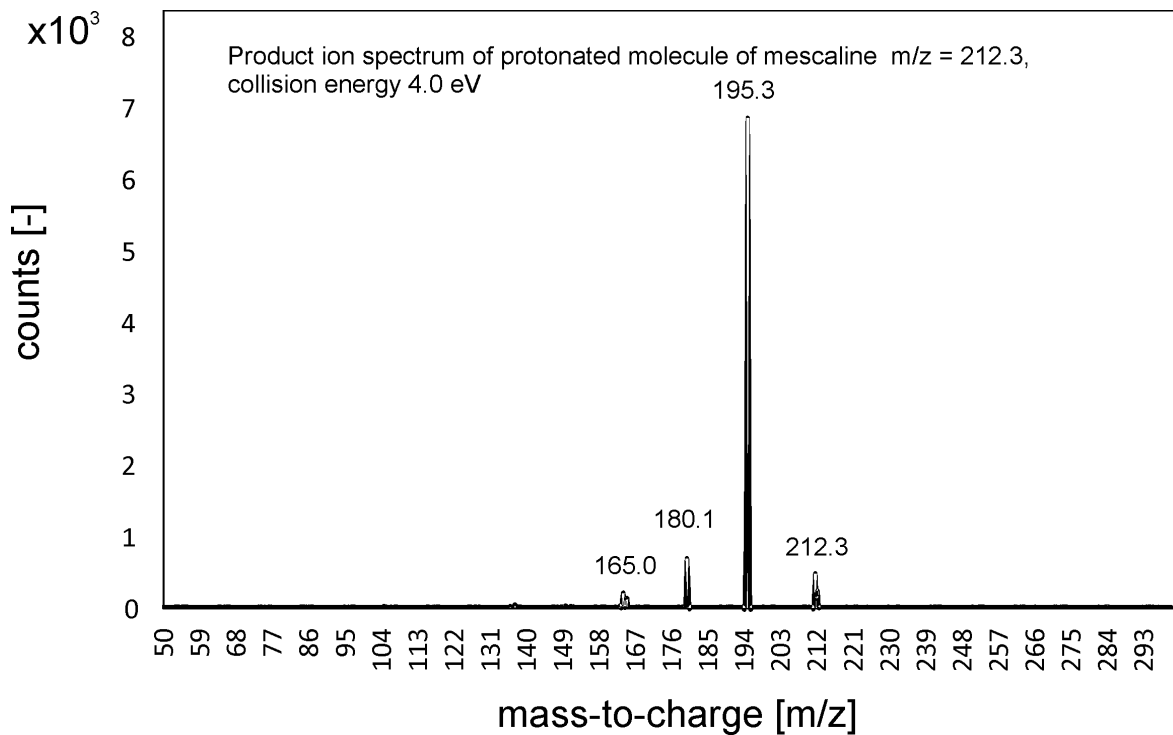
Figure 14: Product ion spectrum measured for a sample of 5 mg/l mescaline in water, collision energy at 4 eV.
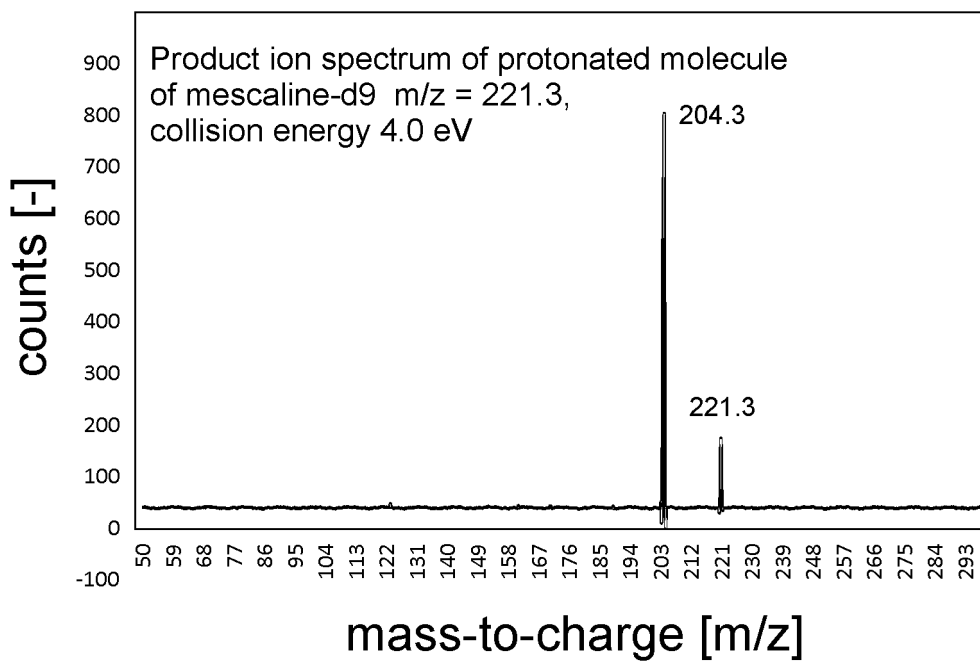
Figure 15: Product ion spectrum measured for a sample of 0.5 mg/l mescaline-d₉ in water, collision energy at 4 eV.

Fragmentor voltage

Fragmentor voltage greatly impacts instrument sensitivity as well as in-source fragmentation. The aim is to find the optimum voltage that produces the highest abundance of the precursor ion as well as the product ions. The most suitable value of the fragmentor voltage is largely dependent on the character of the analyte, as labile analytes can lose several functional groups (such as –OH, -COOH) or significantly decompose in the ion source. Figure 16 clearly shows the optimal value to be 100 V.
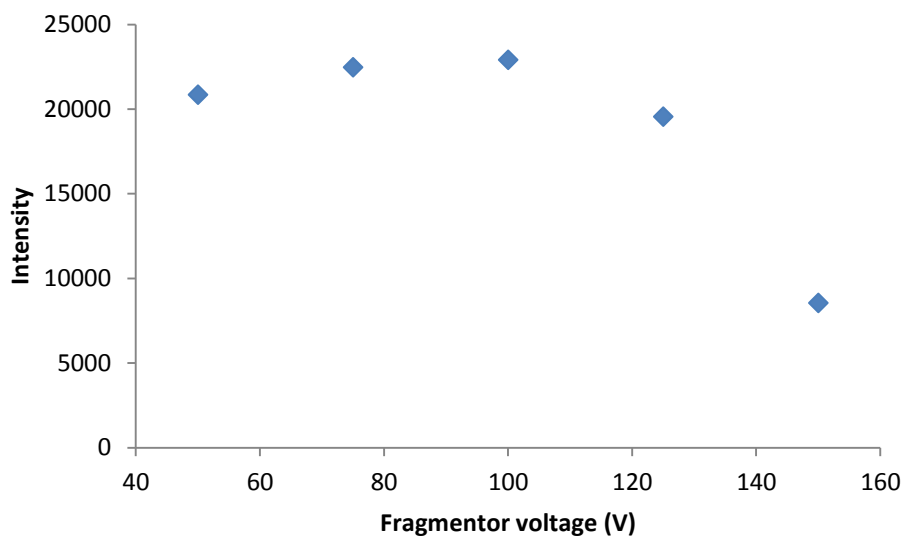
Figure 16: The dependence of intensity on fragmentor voltage, measured for a sample of 5 mg/l mescaline in water.

Gas temperature optimization

The nebulizer gas temperature affects the rate of solvent evaporation and consequently the amount of analyte ions entering the analyser. The influence of gas temperature on intensity, as well as the optimal gas temperature value of 350 °C, can be seen in Figure 17. It is important to note, that the analyte showed no decomposition at this temperature.

Whilst the data shows no plateau, entertaining the possibility of a further increase in peak area with an increase in temperature, 350 °C is the maximal achievable temperature of the instrument.
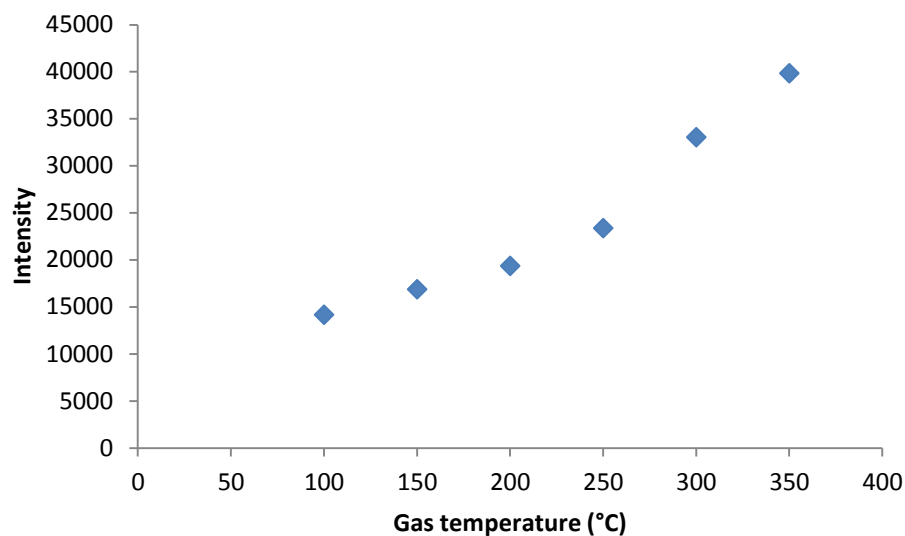
Figure 17: The dependence of intensity on gas temperature, measured for a sample of 5 mg/l mescaline in water.

Sheath liquid composition

The presence of a sheath liquid plays a rather significant role in this experiment as it is needed to compensate for the insufficient flow rate of the eluate from the capillary. For the determination of mescaline in plant and urine samples, methanol (MeOH) and deionised water (W) were chosen to be the main sheath liquid components. Formic acid was added to act as a protonization agent. The relationship between the intensity and the varying sheath liquid composition is presented in Figure 18. Out of the four different tested options, methanol : water : formic acid (50:49.5:0.5% *v/v/v*) seems to be the most sufficient with an acceptable standard deviation.
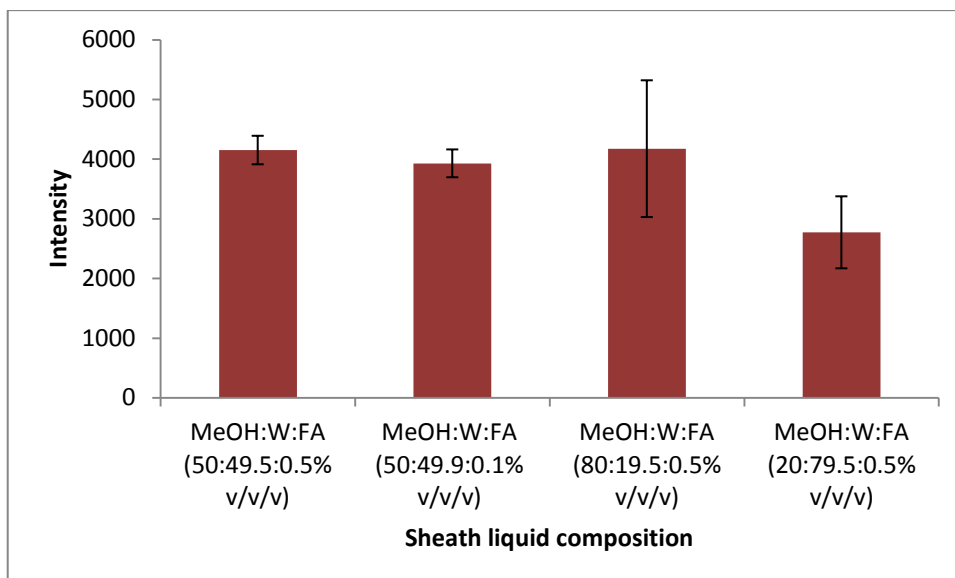
Figure 18: The dependence of intensity on varying sheath liquid composition, measured for a sample of 5 mg/l mescaline in water.

Sheath liquid flow rate optimization

Figure 19 clearly illustrates the relationship between the intensity of the measured sample and the sheath liquid flow. Whilst the 4 μl/min sheath liquid flow, which produces a greater intensity, does have a larger standard deviation compared to the 8 μl/min flow, it is still within an acceptable range (RSD under 5%).
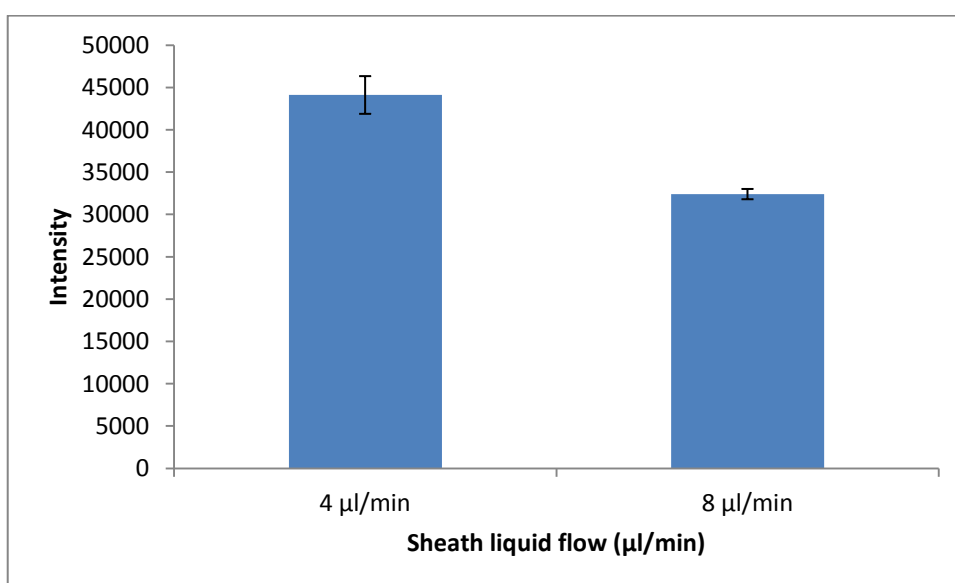
Figure 19: The dependence of intensity on varying sheath liquid flow, measured for a sample of 5 mg/l mescaline in water.

3.4. Method validation

Limit of detection (LOD), Limit of quantification (LOQ)

The limit of detection (LOD) is defined as the lowest concentration of analyte in a sample, which can be detected but not necessarily quantified as an exact value. The LOD was calculated using the signal-to-noise ratio value (SNR = 3) [40]. The limit of quantification (LOQ) is then defined as the lowest concentration of analyte in a sample which can be quantified. The LOD was also calculated using the signal-to-noise ratio value (SNR = 10). Both the LOD and the LOQ for the plant and urine matrix are presented in Table 5.

Linear dynamic range (LDR), Calibration curve parameters

The linear dynamic range for both the plant and the urine samples was determined using a negative matrix adjusted in accordance with the sample preparation procedures (see sections 3.2.1. and 3.2.2.). The negative matrices were spiked with the mescaline and mescaline-d$_9$ standards and measured in the concentration range from 10 to 500 μg/l at six calibration points (10, 25, 50, 100, 250 and 500 μg/l). The concentration of the mescaline-d$_9$ standard was identical in all the calibration samples (50 μg/l). Every calibration point was analysed three times. The calibration curve parameters for the tested matrices are summarised in Table 5.

Due to an unforeseen complication regarding unequal peak areas for the mescaline and mescaline-d$_9$ standards at identical concentration levels, the calibration curve had to be expressed as the dependence of the ratio of the mescaline standard peak area to the mescaline-d$_9$ standard peak area on the concentration of the mescaline standard in the sample.

Table 5: Calibration curve parameters for plant and urine samples.

Matrix type	Calibration curve equation	R	LOD	LOQ
plant	y = 23.411 (± 0.461)x + 0.0384 (± 0.1074)	0.9992	1.30 μg/l	2.06 μg/l
urine	y = 20.565 (± 0.665)x + 0.0247 (± 0.1695)	0.9984	2.13 μg/l	7.11 μg/l

Recovery, matrix effect, process efficiency

An important part of the method validation is the determination of the recovery (RE) of the analyte as well as the matrix effect (ME), allowing an assessment of the reliability and selectivity of the analytical method. Equations 9 and 10 show the process of calculation of matrix effect and recovery, with the symbol A representing the mean peak area of neat standards, B the mean peak area of extracts spiked after extraction and C the mean peak area of extracts spiked before extraction. The relationship between recovery and matrix effect, formulated by equation 11, can be expressed as "process efficiency" (PE) [41].

$$ME\ (\%) = \frac{B}{A} \times 100 \qquad\qquad (9)$$

$$RE\ (\%) = \frac{C}{B} \times 100 \qquad\qquad (10)$$

$$PE\ (\%) = \frac{C}{A} \times 100 = \frac{ME \times RE}{100} \qquad (11)$$

The extraction procedure can be pronounced as suitable under the condition that the analyte recovery is greater than 50%. The acceptable criteria for both the matrix effect and the process efficiency were set at 20%.

For the plant samples, the determination of process efficiency was carried out using two concentration levels (low and high) of the mescaline standard, with the concentration of the mescaline-d_9 standard being identical in both sets. The results are summarised in Table 6.

Table 6: A summary of the recovery, matrix effect and process efficiency for the two different calibration levels of the mescaline standard.

	Low concentration		High concentration	
	Mescaline (0.02 mg/l)	Mescaline-d9 (0.05 mg/l)	Mescaline (0.2 mg/l)	Mescaline-d9 (0.05 mg/l)
ME (%)	83.58 ± 6.63	73.98 ± 14.25	89.94 ± 3.94	102.41 ± 2.64
RE(%)	116.97 ± 7.47	146.65 ± 6.71	109.39 ± 8.91	128.65 ± 7.18
PE(%)	97.76 ± 5.15	108.50 ± 6.41	98.39 ± 4.42	131.75 ± 4.49

Since no extraction procedure was necessary for the determination of mescaline in urine, the recovery of the analyte and process efficiency could not be calculated. The matrix effect values for the urine samples are shown in Table 7.

Table 7: The calculated matrix effect for a sample of mescaline and mescaline-d9 in urine.

	Low concentration		High concentration	
	Mescaline (0.02 mg/l)	Mescaline-d9 (0.05 mg/l)	Mescaline (0.2 mg/l)	Mescaline-d9 (0.05 mg/l)
ME %	89.33 ± 2.64	84.89 ± 4.34	93.15 ± 6.84	88.75 ± 5.81

Accuracy (bias)

The term accuracy (bias) is defined as "the difference between the expectation of the test results and an accepted reference value" and is often expressed as the percentage deviation from the accepted value, which was set at ± 15% (±20% near LOD) [40]. The experiment was performed at two concentration levels, low (0.02 of mg/l mescaline) and high (0.2 mg/l of mescaline), for both the plant matrix and urine. The results were calculated using the calibration curve equations and are summarised in Table 8.

Table 8: Calculated percentage bias values for two concentration levels (0.02 mg/l and 0.2 mg/l) of mescaline in plant and urine.

	BIAS %	
	Low concentration (0.02 mg/l mescaline)	High concentration (0.2 mg/l mescaline)
Negative plant matrix	15.00	-0.18
10x diluted urine	28.77	-0.33

Since the urine samples were not extracted, merely diluted, the metabolic interferences seem to have caused a higher percentage bias than would be acceptable.

Repeatability

The samples of the mescaline and mescaline-d_9 standards in varying matrices were measured six times within one workday to establish intra-day repeatability. The measurements were repeated for five consecutive days to obtain the inter-day repeatability values. The acceptable criteria were set at 10% RSD. The repeatability values for the plant and urine samples can be seen in Table 9.

Table 9: Intra-day and inter-day repeatability measured for a sample containing 0.2 mg/l of mescaline and 0.05 mg/l of mescaline-d_9 in varying matrices.

Standards in water		
	Intra-day repeatability	Inter-day repeatability
Peak area ratio RSD (%)	5.74	4.41
Mescaline migration time RSD (%)	1.16	0.66
Mescaline-d9 migration time RSD (%)	1.12	0.67

Standards in negative plant matrix spiked after extraction		
	Intra-day repeatability	Inter-day repeatability
Peak area ratio RSD (%)	3.61	5.31
Mescaline migration time RSD (%)	0.84	3.51
Mescaline-d9 migration time RSD (%)	1.30	0.31

Standards in negative plant matrix spiked before extraction		
	Intra-day repeatability	Inter-day repeatability
Peak area ratio RSD (%)	2.51	2.95
Mescaline migration time RSD (%)	0.44	1.43
Mescaline-d9 migration time RSD (%)	0.44	1.44

Standards in 10x diluted urine		
	Intra-day repeatability	Inter-day repeatability
Peak area ratio RSD (%)	5.44	0.19
Mescaline migration time RSD (%)	0.53	2.22
Mescaline-d9 migration time RSD (%)	0.55	2.24

The study of thermal decomposition of mescaline during sample preparation

Model samples of mescaline at two concentration levels, 0.02 mg/l (low) and 0.2 mg/l (high) were dried at 105°C to ascertain whether the mescaline in plant samples undergoes thermal decomposition (a loss of the amine group) during the sample preparation process. Three parallel samples for each concentration were analyzed and compared to a fourth sample (that has not been exposed to the high temperature).

The low concentration level sample shows a 14.94% loss of analyte, while the high concentration level sample shows a 22.72% loss of analyte. This undesired phenomenon could possibly be avoided in future experiments by utilizing a lyophilizer instead of an oven.

4. Results and discussion

The optimized and validated method was utilized for the determination of mescaline in real samples. The plant samples donated by the Department of Botany were of cacti grown artificially out of their natural habitat, the majority of which were samples of *Lophophora williamsii* (WILL), with a few samples of *Lophophora alberto-vojtechii* (ALV) and one sample of *Lophophora fricii* (FRI). Both ALV and FRI are cacti with an identical genotype to that of *Lophophora*. The calibration curve method was used for the quantification of mescaline in both the plant and urine samples. Examples of the reconstructed electropherograms are shown in Figures 20 and 21.
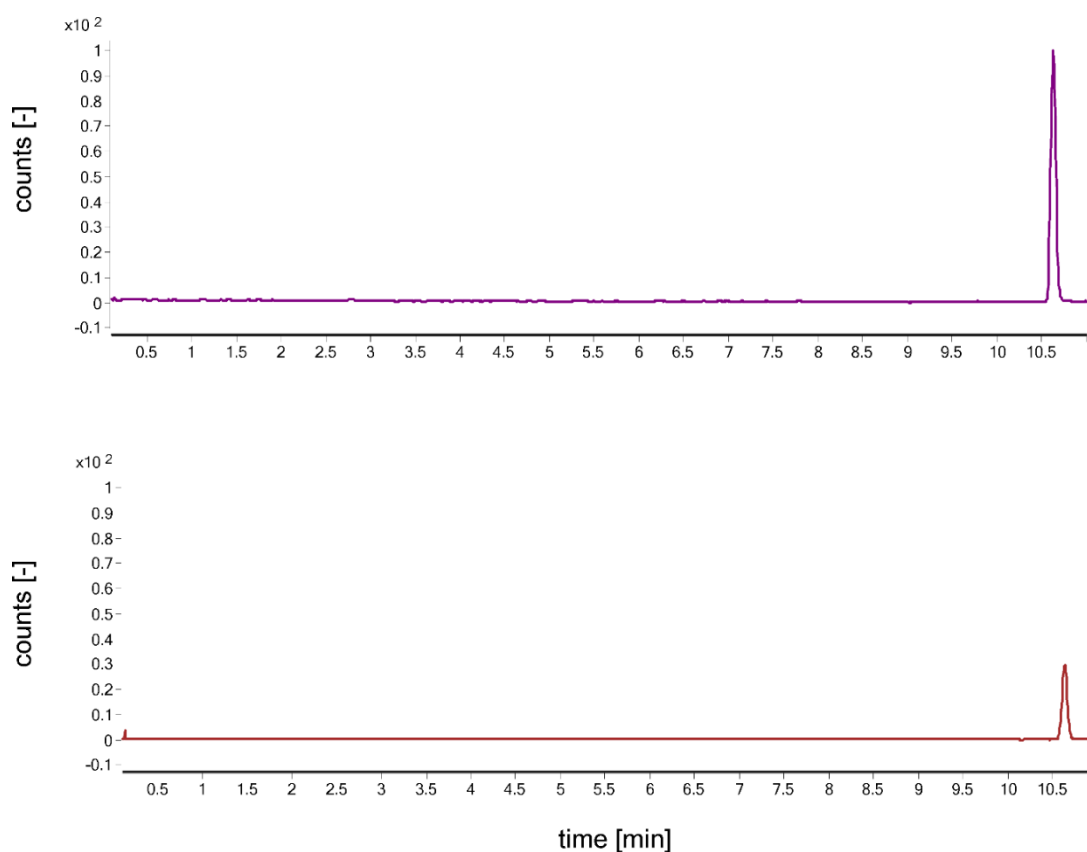
Figure 20: Real plant sample (WILL 8B) (A) The electropherogram of mescaline (unknown concentration) in plant sample (B) The electropherogram of mescaline-d_9 (0.05 mg/l) in plant sample.
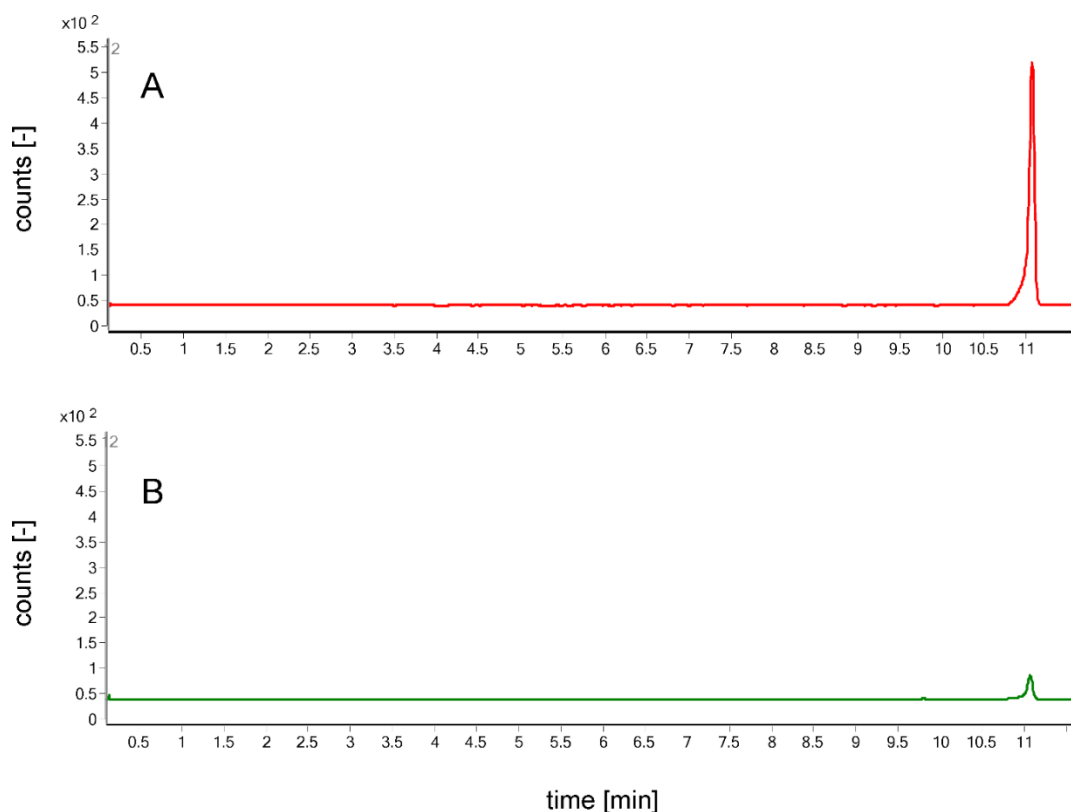
Figure 21: Spiked sample of urine containing the mescaline and mescaline-d9 standards (A) The electropherogram of mescaline (0.5 mg/l) in urine (B) The electropherogram of mescaline-d_9 (0.05 mg/l) in urine.

A clear difference in peak shape can be observed when comparing the spiked urine sample, Figure 21A, to the sample of mescaline extracted from plant material, Figure 20A. Since the urine was merely diluted, the undoubtedly high amount of various salts and metabolites in the sample are most definitely the cause of the fronting peak shape.

Table 10 summarizes the measured amounts of mescaline (μg/g of dried cactus) in the individual samples, together with their approximate location of origin and federal state (if known). The mescaline content for the samples of *Lophophora williamsii* (WILL) covers a wide range from 5640.22 ± 207.84 μg/g (WILL 13A) to under the limit of detection (WILL 33B). As was expected, only very small amounts (<15μg/g of dried cactus) of mescaline were found in the *Lophophora alberto-vojtechii* (ALV) and the *Lophophora fricii* (FRI) samples. The approximate location distribution of the analyzed samples is illustrated in Figure 22.

Table 10: Total amount of mescaline in studied plant material expressed as μg of mescaline per g of dried plant.

Sample ID	μg/g	Approx. Locality	Federal state
ALV 4B	2.66 ± 0.38	Parida	San Luis Potosí (S.L.P.)
ALV 16B	<LOD	N/A[2]	
ALV 16F	1.64 ± 0.10	N/A	
ALV 24A	<LOD	Vanegas	San Luis Potosí (S.L.P.)
ALV 24C	<LOD	Vanegas	San Luis Potosí (S.L.P.)
ALV 30B	3.45 ± 0.38	N/A	Nuevo León (N.L.)
WILL 1B	136.61 ± 11.27	Tecolotes	Zacatecas (Zac.)
WILL 2A	40.49 ± 3.45	Milagro Huizache	San Luis Potosí (S.L.P.)
WILL 2B	40.49 ± 3.45	Milagro Huizache	San Luis Potosí (S.L.P.)
WILL 6A	506.58 ± 59.91	Hipolito	Coahuila (Coah.)
WILL 8B	171.42 ± 10.26	Boňuelos	Coahuila (Coah.)
WILL 13A	5640.22 ± 207.84	Estanqe Nuevo	Nuevo León (N.L.)
WILL 18B	2710.63 ± 7.72	San Ignacio de Texas	Nuevo León (N.L.)
WILL 20A	769.39 ± 82.66	El Tulillo Cardona	Zacatecas (Zac.)
WILL 20D	769.39 ± 82.66	El Tulillo Cardona	Zacatecas (Zac.)
WILL 21	787.35 ± 61.49	Las Cruces	San Luis Potosí (S.L.P.)
WILL 25A	376.72 ± 36.24	Los Colorados	Coahuila (Coah.)
WILL 33B	<LOD	Sabana Grande	Zacatecas (Zac.)
WILL 34A	10.26 ± 1.28	Valecitos	Nuevo León (N.L.)
WILL 36A	119.60 ± 3.62	Guzman	Coahuila (Coah.)
WILL 39A	<LOD	San Ignacio de Texas	Nuevo León (N.L.)
WILL 45A	<LOD	N/A	San Luis Potosí (S.L.P.)
WILL 48A	35.86 ± 4.61	San Felipe de Teyra	Zacatecas (Zac.)
WILL 49A	1653.18 ± 15.52	Los Colorados	Coahuila (Coah.)
WILL 50B	47.78 ± 5.90	Valejos Huizache	San Luis Potosí (S.L.P.)
WILL 53B	3098.89 ± 143.62	near Garambullo	Coahuila (Coah.)
WILL 57C	<LOD	Sabana Grande	Zacatecas (Zac.)
WILL 59	5.81 ± 0.43	N/A	
WILL 63	333.83 ± 28.70	Rancho Negro	Chihuahua (Chih.)
WILL 65	7.03 ± 0.83	Del Rio	Texas (USA)
FRI 3	12.94 ± 1.90	N/A	

---

[2] N/A – information regarding locality not provided
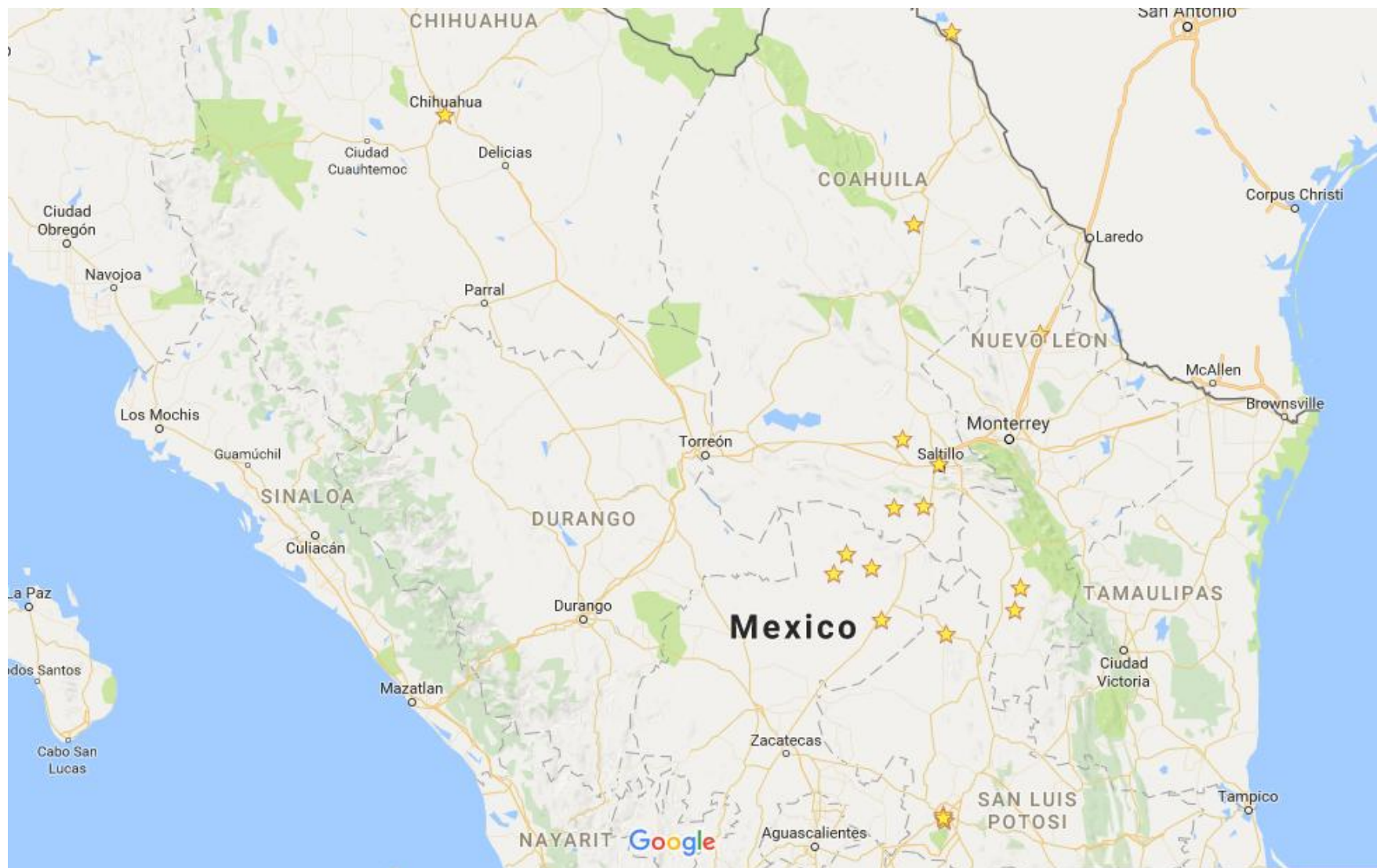
Figure 22: An approximate location distribution of the analysed samples (localities marked by a star).

5. Conclusion

A new method for the identification and quantification of mescaline in plant and biological matrices, using CE-ESI-MS, was developed. The aim of this thesis was to create a fast, easy and effective alternative to the existing chromatographic methods. The analyses were carried out using a 25 mM ammonium acetate buffer with pH adjusted to 3.5. The experimental parameters were optimized in order to gain the best selectivity, resolution, accuracy (bias) and repeatability values. The recovery and matrix effect were studied to validate the simple extraction procedure for the plant samples. As the urine samples were not extracted, merely diluted; only the matrix effect could be determined. The limits of detection for both matrices are comparable to the chromatographic methods.

The hallucinogenic doses of mescaline typically range from 200 to 500 mg of the drug. Since the highest concentration of mescaline in the plant samples was determined to be about 5.6 mg/g (5640.22 ± 207.84 μg/g) of dried cactus, the actual amount of plant matter that would have to be ingested to cause any of the desired symptoms is unrealistic. Moreover, the stated concentration value could be considered an outlier, as the majority of the analysed plant samples contained concentrations at least an order of magnitude lower. The low content of mescaline in the samples is likely caused by the plants being grown artificially out of their natural habitat.

6. References

[1]   J. Beyer, O. H. Drummer, and H. H. Maurer, "Analysis of toxic alkaloids in body samples," *Forensic Science International*, vol. 185, no. 1–3, pp. 1–9, 2009.

[2]   K. Bjornstad, A. Helander, and O. Beck, "Development and clinical application of an LC-MS-MS method for mescaline in urine.," *Journal of analytical toxicology*, vol. 32, no. 3, pp. 227–231, 2008.

[3]   "National Center for Biotechnology Information," *PubChem Compound Database*. [Online]. Available: http://www.ncbi.nlm.nih.gov/. [Accessed: 28-Aug-2016].

[4]   R. Casado, I. Uriarte, R. Y. Cavero, and M. I. Calvo, "LC-PAD determination of mescaline in cactus 'peyote' (Lophophora williamsii)," *Chromatographia*, vol. 67, no. 7–8, pp. 665–667, 2008.

[5]   J. H. Halpern, "Hallucinogens and dissociative agents naturally growing in the United States," *Pharmacology and Therapeutics*, vol. 102, no. 2, pp. 131–138, 2004.

[6]   J. H. Halpern, A. R. Sherwood, J. I. Hudson, D. Yurgelun-Todd, and H. G. Pope, "Psychological and cognitive effects of long-term peyote use among Native Americans," *Biological Psychiatry*, vol. 58, no. 8, pp. 624–631, 2005.

[7]   A. L. Halberstadt, S. B. Powell, and M. A. Geyer, "Role of the 5-HT2A receptor in the locomotor hyperactivity produced by phenylalkylamine hallucinogens in mice," *Neuropharmacology*, vol. 70, pp. 218–227, 2013.

[8]   M. Franco-Molina, R. Gomez-Flores, P. Tamez-Guerra, R. Tamez-Guerra, L. Castillo-Leon, and C. Rodríguez-Padilla, "In vitro Immunopotentiating Properties and Tumour Cell Toxicity Induced by Lophophora williamsii (Peyote) Cactus Methanolic Extract," *Phytotherapy Research*, vol. 17, no. 9, pp. 1076–1081, 2003.

[9]   J. L. Henry, J. Epley, and T. P. Rohrig, "The analysis and distribution of mescaline in postmortem tissues," *Journal of analytical toxicology*, vol. 27, no. September, pp. 381–382, 2003.

[10]   C. Gambelunghe, R. Marsili, K. Aroni, M. Bacci, and R. Rossi, "GC-MS and GC-MS/MS in PCI Mode Determination of Mescaline in Peyote Tea and in Biological Matrices," *Journal of Forensic Sciences*, vol. 58, no. 1, pp. 270–278, 2013.

[11]   B. Prue, "Prevalence of reported peyote use 1985-2010 effects of the American Indian Religious Freedom Act of 1994," *American Journal on Addictions*, vol. 23, no. 2, pp. 156–161, 2014.

[12]   H. R. El-Seedi, P. A. G. M. De Smet, O. Beck, G. Possnert, and J. G. Bruhn, "Prehistoric peyote use: Alkaloid analysis and radiocarbon dating of archaeological specimens of Lophophora from Texas," *Journal of Ethnopharmacology*, vol. 101, no. 1–3, pp. 238–242, 2005.

[13]   M. T. Klein, M. Kalam, W. Street, and M. Terry, "Mescaline concentrations in three principal tissues of Lophophora williamsii (Cactaceae): implications for sustainable harvesting practices," *Haseltonia*, vol. 20, pp. 34–42, 2015.

[14]   M. Terry, "Stalking the wild Lophophora: Part 3 San Luis Potosí (central), Querétaro, and Mexico City," *Cactus and Succulent Journal*, vol. 80, no. 6, pp.

310–317, 2008.

[15] H. Rosengarten and a J. Friedhoff, "A review of recent studies of the biosynthesis and excretion of hallucinogens formed by methylation of neurotransmitters or related substances.," *Schizophrenia bulletin*, vol. 2, pp. 90–105, 1976.

[16] R. B. Herbert, *The Biosynthesis of Secondary Metabolites*. Chapman & Hall, 1989.

[17] V. Habrdova, F. T. Peters, D. S. Theobald, and H. H. Maurer, "Screening for and validated quantification of phenethylamine-type designer drugs and mescaline in human blood plasma by gas chromatography/mass spectrometry," *Journal of Mass Spectrometry*, vol. 40, no. 6, pp. 785–795, 2005.

[18] H. J. Helmlin and R. Brenneisen, "Determination of psychotropic phenylalkylamine derivatives in biological matrices by high-performance liquid chromatography with photodiode-array detection," *Journal of Chromatography*, vol. 593, no. 1–2, pp. 87–94, 1992.

[19] J. L. Valentine and R. Middleton, "GC-MS identification of sympathomimetic amine drugs in urine: rapid methodology applicable for emergency clinical toxicology.," *Journal of analytical toxicology*, vol. 24, no. 3, pp. 211–22, 2000.

[20] M. Sergi, D. Compagnone, R. Curini, G. D'Ascenzo, M. Del Carlo, S. Napoletano, and R. Risoluti, "Micro-solid phase extraction coupled with high-performance liquid chromatography-tandem mass spectrometry for the determination of stimulants, hallucinogens, ketamine and phencyclidine in oral fluids.," *Analytica chimica acta*, vol. 675, no. 2, pp. 132–7, 2010.

[21] U. Backofen, F. M. Matysik, W. Hoffmann, and C. E. Lunte, "Analysis of illicit drugs by nonaqueous capillary electrophoresis and electrochemical detection," *Fresenius' Journal of Analytical Chemistry*, vol. 367, no. 4, pp. 359–363, 2000.

[22] M. C. Gennaro, E. Gioannini, D. Giacosa, and D. Siccardi, "Determination of mescaline in hallucinogenic Cactaceae by ion- interaction HPLC," *Analytical Letters*, vol. 29, no. 13. pp. 2399–2409, 1996.

[23] S. a Sweeney, R. C. Kelly, J. a Bourland, T. Johnson, W. C. Brown, H. Lee, and E. Lewis, "Amphetamines in hair by enzyme-linked immunosorbent assay.," *Journal of analytical toxicology*, vol. 22, no. October, pp. 418–424, 1998.

[24] J. Frenz and W. S. Hancock, "High performance capillary electrophoresis.," *Trends in biotechnology*, vol. 9, no. 7, pp. 243–250, 1991.

[25] A. Prange and D. Pröfrock, "Application of CE-ICP-MS and CE-ESI-MS in metalloproteomics: Challenges, developments, and limitations," *Analytical and Bioanalytical Chemistry*, vol. 383, no. 3, pp. 372–389, 2005.

[26] B. Bower, K. Kodama, B. Swanson, T. Fowler, H. Meerman, K. Collier, C. Mitchinson, and M. Ward, "Introduction to Capillary Electrophoresi," *Carbohydrases from Trichoderma reesei and other micro-organisms*, pp. 327–334, 1998.

[27] D. Harvey, "Modern Analytical Chemistry," *Modern Analytical Chemistry*, vol. 1, p. 817 pages, 2000.

[28] V. Kašička, "Teoretické základy a separační principy kapilárních electromigračních metod," *Chem. listy*, vol. 91, pp. 320–329, 1997.

[29] D. Heiger, "High performance capillary electrophoresis," *High Performance Capillary Electrophoresis*, pp. 17–24, 2000.

[30]   H. Whatley, "Basic principles and modes of capillary electrophoresis," *Clinical and Forensic Applications of Capillary Electrophoresis*, pp. 21–58, 2001.

[31]   J. P. Landers, *Handbook of capillary and microchip electrophoresis and associated microtechniques (2nd Edn.)*. CRC Press LLC, 1997.

[32]   J. Ohnesorge, C. Neusüß, and H. Wätzig, "Quantitation in capillary electrophoresis-mass spectrometry," *Electrophoresis*, vol. 26, no. 21, pp. 3973–3987, 2005.

[33]   A. Von Brocke, G. Nicholson, and E. Bayer, "Recent advances in capillary electrophoresis/electrospray-mass spectrometry," *Electrophoresis*, vol. 22, no. 7, pp. 1251–1266, 2001.

[34]   P. Schmitt-Kopplin and M. Frommberger, "Capillary electrophoresis-mass spectrometry: 15 years of developments and applications.," *Electrophoresis*, vol. 24, no. 22–23, pp. 3837–3867, 2003.

[35]   E. J. Maxwell and D. D. Y. Chen, "Twenty years of interface development for capillary electrophoresis-electrospray ionization-mass spectrometry," *Analytica Chimica Acta*, vol. 627, no. 1, pp. 25–33, 2008.

[36]   A. Technologies, "Agilent 6100 Series Quadrupole LC/MS Systems Concepts Guide," *Agilent Technologies*, vol. Revision A, p. 126, 2011.

[37]   I. Bull, "Bristol University - Gas Chromatography Mass Spectrometry (GC/MS)." [Online]. Available: http://www.bris.ac.uk/nerclsmsf/techniques/gcms.html. [Accessed: 25-Mar-2017].

[38]   E. De Hoffmann and V. Stroobant, *Mass Spectrometry - Priniples and Applications.*, vol. 29, no. 6. 2007.

[39]   O. Ogunbodede, D. McCombs, K. Trout, P. Daley, and M. Terry, "New mescaline concentrations from 14 taxa/cultivars of Echinopsis spp. (Cactaceae) (' San Pedro') and their relevance to shamanic practice," *Journal of Ethnopharmacology*, vol. 131, pp. 356–362, 2010.

[40]   F. T. Peters, O. H. Drummer, and F. Musshoff, "Validation of new methods," *Forensic Science International*, vol. 165, no. 2–3, pp. 216–224, 2007.

[41]   B. K. Matuszewski, M. L. Constanzer, and C. M. Chavez-Eng, "Strategies for the assessment of matrix effect in quantitative bioanalytical methods based on HPLC-MS/MS," *Analytical Chemistry*, vol. 75, no. 13, pp. 3019–3030, 2003.

7. Abbreviations

ALV	*Lophophora alberto-vojtechii*
APCI	atmospheric pressure chemical ionization
APPI	atmospheric pressure photoionization
CE	capillary electrophoresis
DAD	diode array detector
EC	electrochemical (detector)
EI	electron ionization
ELISA	enzyme-linked immunosorbent assay
EOF	electroosmotic flow
ESI	electrospray ionisation
FA	formic acid
FRI	*Lophophora fricii*
GC	gas chromatography
HCl	hydrochloric acid
He	helium
HFBA	heptafluorobutyric anhydride
kV	kilovolts
LC (HPLC)	(high performance) liquid chromatography
LDR	linear dynamic range
LLE	liquid-liquid extraction
LOD	limit of detection
LOQ	limit of quantification
LSD	lysergic acid diethylamide
MALDI	matrix-assisted laser desorption ionization
ME	matrix effect
MeOH	methanol
MRM	multiple reaction monitoring
MS	mass spectrometry

NAC	Native American Church
NACE	non-aqueous capillary electrophoresis
PAD	photodiode array detector
PE	process efficiency
PFPA	pentafluoropropionic anhydride
PFPOH	pentafluoropropanol
pKa	acid dissociation constant (logarithmic)
Pt	platinum
QqQ	triple quadrupole
RE	recovery
RP	reverse phase
RSD	relative standard deviation
SIM	selected ion monitoring
SNR	signal-to-noise ratio
SRM	selected reaction monitoring
SPE	solid phase extraction
STD	standard
T gradient	temperature gradient
TLC	thin layer chromatography
US	United States
UV	ultraviolet (detector)
W	water
WILL	*Lophophora williamsii*